JCB Article

Real-time single cell analysis of Smac/DIABLO release during apoptosis

Markus Rehm,[1,2] Heiko Düßmann,[1] and Jochen H.M. Prehn[1,2]

[1]Interdisciplinary Center for Clinical Research, Research Group "Apoptosis and Cell Death", University Münster Clinics, D-48149 Münster, Germany
[2]Center for Neurology and Neurosurgery, Experimental Neurosurgery, Johann Wolfgang Goethe-University Clinics, D-60590 Frankfurt, Germany

We examined the temporal and causal relationship between Smac/DIABLO release, cytochrome *c* (cyt-*c*) release, and caspase activation at the single cell level during apoptosis. Cells treated with the broad-spectrum caspase inhibitor z-VAD-fmk, caspase-3 (Casp-3)–deficient MCF-7 cells, as well as Bax-deficient DU-145 cells released Smac/DIABLO and cyt-*c* in response to proapoptotic agents. Real-time confocal imaging of MCF-7 cells stably expressing Smac/DIABLO-yellow fluorescent protein (YFP) revealed that the average duration of Smac/DIABLO-YFP release was greater than that of cyt-*c*-green fluorescent protein (GFP). However, there was no significant difference in the time to the onset of release, and both cyt-*c*-GFP and Smac/DIABLO-YFP release coincided with mitochondrial membrane potential depolarization. We also observed no significant differences in the Smac/DIABLO-YFP release kinetics when z-VAD-fmk–sensitive caspases were inhibited or Casp-3 was reintroduced. Simultaneous measurement of DEVDase activation and Smac/DIABLO-YFP release demonstrated that DEVDase activation occurred within 10 min of release, even in the absence of Casp-3.

Introduction

During apoptosis, mitochondria increase their membrane permeability (Martinou and Green, 2001). Several proteins that normally reside in the intermembrane and intracristal space are released during this process. The release of cytochrome *c* (cyt-*c*) triggers the formation of a multiprotein complex, the apoptosome (Liu et al., 1996). This complex is composed of apoptotic protease-activating factor 1, procaspase-9, dATP, and cyt-*c* (Li et al., 1997; Zou et al., 1997). Apoptosome formation results in the activation of executioner caspases including caspase-3 (Casp-3), -6, and -7 (Li et al., 1997; Slee et al., 1999; Zou et al., 1997). The loss of cyt-*c* simultaneously initiates a mitochondrial organelle dysfunction program that is characterized by inner mitochondrial membrane potential ($\Delta\Psi_M$) depolarization, ATP depletion, and free radical production (Zamzami et al., 1995; Adachi et al., 1997; Cai and Jones, 1998; Heiskanen et al., 1999; Mootha et al., 2001; Waterhouse et al., 2001; Madesh et al., 2002; Dussmann et al., 2003a,b).

Inhibitor of apoptosis proteins (IAPs) are believed to be naturally occurring inhibitors of caspase activation (Holcik and Korneluk, 2001). During apoptosis, two other proteins are released from mitochondria that facilitate apoptosome formation by neutralizing the antiapoptotic activity of IAPs: the second mitochondria-derived activator of caspase/direct IAP binding protein with low pI (Smac/DIABLO) and Omi/HtrA2, the mammalian homologue of the *Escherichia coli* heat shock–inducible protein HtrA (Du et al., 2000; Verhagen et al., 2000; Suzuki et al., 2001; Hegde et al., 2002; Martins et al., 2002; Verhagen et al., 2002). Both proteins bind IAPs by direct interaction within specific domains designated BIR domains.

Interestingly, the release of both cyt-*c* and Smac/DIABLO has been shown to be a prerequisite for apoptotic cell death in several model systems, such as nerve growth factor deprivation–induced cell death of sympathetic neurons and anticancer drug-induced tumor cell death (Deshmukh et al., 2002; Fulda et al., 2002; Hunter et al., 2003). However, despite the importance of Smac/DIABLO release for various cell death

Address correspondence to Jochen H.M. Prehn, Experimental Neurosurgery Center for Biological Chemistry (ZBC), HS 25 B, 4. OG, Johann Wolfgang Goethe-University Clinics, Theodor-Stern-Kai 7, D-60590 Frankfurt, Germany. Tel.: 49-69-6301-6930. Fax: 49-69-6301-5575. email: prehn@rcsi.ie

Key words: mitochondria; cytochrome *c*; caspases; confocal microscopy; fluorescence resonance energy transfer

Abbreviations used in this paper: Casp-3, caspase-3; CHX, cycloheximide; cyt-*c*, cytochrome *c*; $\Delta\Psi_M$, inner mitochondrial membrane potential; Eto, etoposide; FRET, fluorescence resonance energy transfer; IAP, inhibitor of apoptosis protein; STS, staurosporine; TMRM, tetramethyl rhodamine methyl ester; z-VAD-fmk, z-Val-Ala-Asp(*O*-methyl)-fluoromethylketone.

The Journal of Cell Biology, Volume 162, Number 6, September 15, 2003 1031–1043
http://www.jcb.org/cgi/doi/10.1083/jcb.200303123

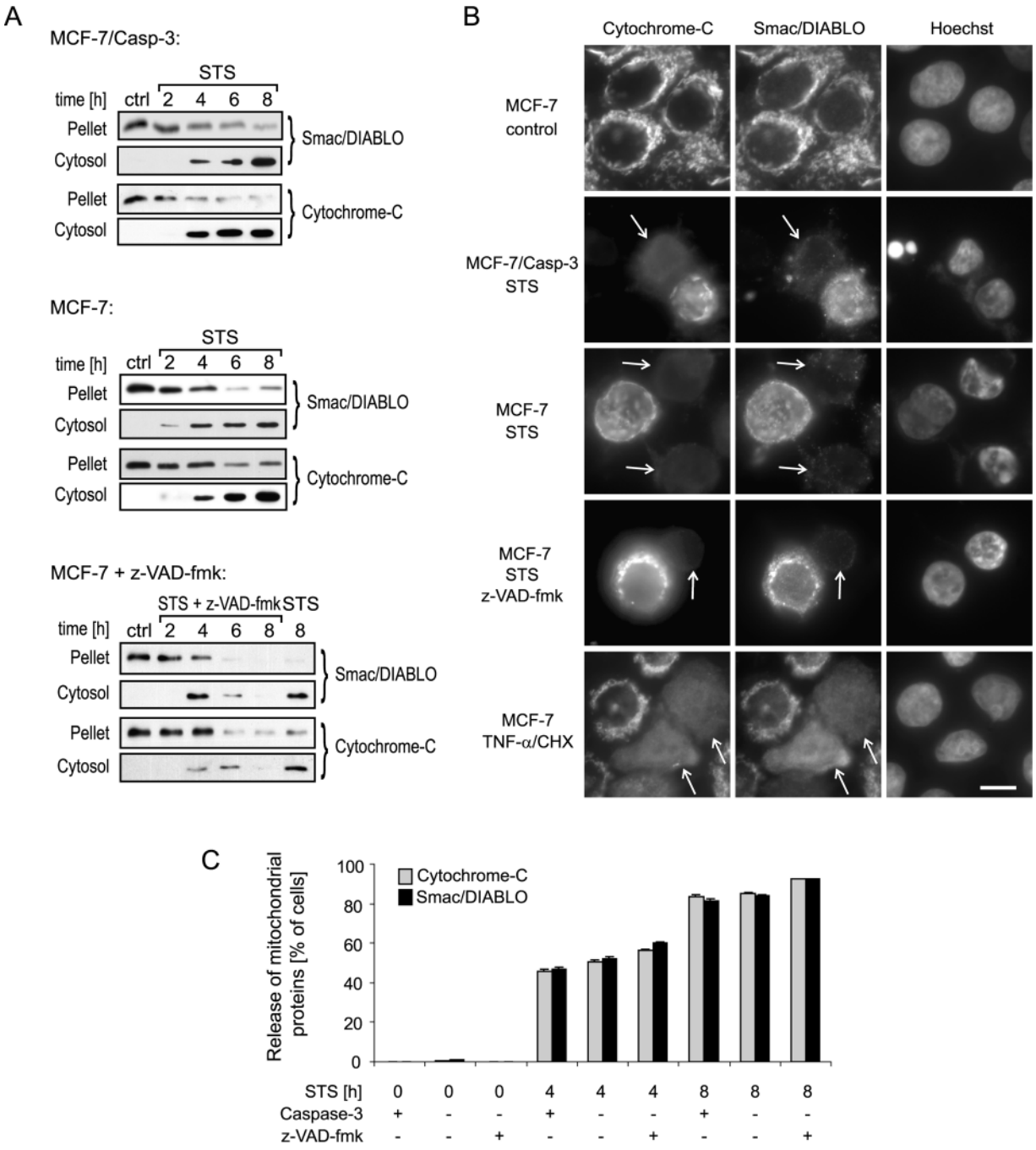

Figure 1. **Comparison of Smac/DIABLO and cyt-*c* release during apoptosis: effect of Casp-3 and z-VAD-fmk–sensitive caspases.** (A) MCF-7/Casp-3 cells and MCF-7 cells were treated with 3 μM STS or 3 μM STS plus 200 μM of the broad-spectrum caspase inhibitor z-VAD-fmk for the indicated time periods. Release of Smac/DIABLO and cyt-*c* from the mitochondria-containing pellet fractions into the cytosol was analyzed by Western blotting. Controls were treated with DMSO. Experiments were repeated twice with similar results. (B) Immunofluorescence analysis showing the redistribution of cyt-*c* and Smac/DIABLO during apoptosis. Cells were treated with 3 μM STS, 3 μM STS plus 200 μM z-VAD-fmk or 200 ng/ml, and 1 μg/ml TNF-α/CHX for 6 h. Control cells received vehicle (DMSO). Arrows indicate cells that show a cyt-*c* and Smac/DIABLO redistribution in response to the agents. Nuclear morphology was detected by Hoechst staining. Bar, 10 μm. (C) Quantification of cells showing cyt-*c* or Smac/DIABLO release as judged by immunofluorescence analysis. MCF-7/Casp-3 cells (indicated as Casp-3 +) were treated with 3 μM STS. MCF-7 cells (indicated as Casp-3 −) were treated with 3 μM STS in the presence or absence of 200 μM z-VAD-fmk. Data were collected from $n = 200–300$ cells per treatment in 11–14 randomly selected image frames from $n = 3$ independent experiments. There was no statistically significant difference between the three treatment groups or between cyt-*c* and Smac/DIABLO release at any time point investigated. Error bars equal SEM.

paradigms, the mechanism of Smac/DIABLO release during apoptosis is not fully characterized. Indeed, controversial data exist in the literature as to whether the release of Smac/DIABLO requires or actually precedes caspase activation (Adrain et al., 2001; Chauhan et al., 2001; Zhang et al., 2001). Moreover, little is known about the temporal and causal relationship between Smac/DIABLO release and cyt-*c* release, mitochondrial dysfunction, and effector caspase activation at

the single cell level. To address these questions, we used real-time single cell analyses in combination with well-established model systems, HeLa cells, and the Casp-3–deficient MCF-7 breast adenocarcinoma cell line (Janicke et al., 1998).

Results

Release of Smac/DIABLO from mitochondria during apoptosis can occur independent of Casp-3 and z-Val-Ala-Asp(*O*-methyl)-fluoromethylketone (z-VAD-fmk)–sensitive caspases

We investigated the process of Smac/DIABLO and cyt-*c* release during apoptosis in Casp-3–deficient MCF-7 cells and MCF-7 cells stably transfected with Casp-3 (MCF-7/Casp-3; Janicke et al., 1998). Exposure of MCF-7/Casp-3 cells to proapoptotic agents such as staurosporine (STS), etoposide (Eto), or TNF-α plus cycloheximide (TNF-α/CHX) results in an efficient activation of effector caspases that is followed in ~30 min by cell shrinkage, membrane blebbing, chromatin condensation, and DNA fragmentation (Janicke et al., 1998; Luetjens et al., 2001; Rehm et al., 2002). In contrast, due to the lack of Casp-3, effector caspase activation sets in slower and less efficient in MCF-7 cells and is largely mediated by caspase-7 (Cuvillier et al., 2001; Liang et al., 2001; Rehm et al., 2002). Cell shrinkage is delayed by ~120 min, and cell death sets in without oligonucleosomal DNA fragmentation (Janicke et al., 1998; Rehm et al., 2002). We activated the mitochondrial apoptosis pathway in both cell types by addition of 3 μM of the protein kinase inhibitor STS. Selective plasma membrane permeabilization and subsequent immunoblotting revealed that cyt-*c* and Smac/DIABLO were both released from mitochondria and accumulated in the cytosol after 4 h of STS treatment, independent of the presence or absence of Casp-3 (Fig. 1 A). Similar results were obtained in MCF-7 and MCF-7/Casp-3 cells after treatment with submaximal STS concentrations (0.1 μM) or after stimulation of death receptors with TNF-α/CHX (unpublished data).

A previous report has demonstrated that the broad-spectrum caspase inhibitor z-VAD-fmk inhibited the accumulation of Smac/DIABLO in the cytosol during apoptosis (Adrain et al., 2001). MCF-7 cells treated with STS and 200 μM z-VAD-fmk indeed showed a significantly reduced accumulation of Smac/DIABLO in the cytosol, particularly at later time points. This effect was also detectable in the case of cyt-*c*. However, neither Smac/DIABLO nor cyt-*c* release was significantly influenced by the caspase inhibitor as judged by a decrease in Smac/DIABLO and cyt-*c* in the mitochondria-containing pellet fraction comparable to that seen after STS-only treatment (Fig. 1 A).

These results were confirmed by immunofluorescence analysis of Smac/DIABLO and cyt-*c* distribution during apoptosis. MCF-7 and MCF-7/Casp-3 cells were treated with 3 μM STS for 6 h, either in the absence or presence of 200 μM z-VAD-fmk. Cells were fixed, immunostained for Smac/DIABLO and cyt-*c*, and analyzed by fluorescence microscopy. Fig. 1 B demonstrates changes in the Smac/DIABLO and cyt-*c* signals in response to STS in MCF-7 and MCF-7/Casp-3 cells. We noted a concomitant decrease in the mitochondrial Smac/DIABLO and cyt-*c* immunofluorescence signals in individual MCF-7 and MCF-7/Casp-3 cells during the STS treatment (Fig. 1 B), suggesting that the two proteins were coreleased during apoptosis. Similar results were obtained in STS plus z-VAD-fmk–treated MCF-7 cells (Fig. 1 B). The

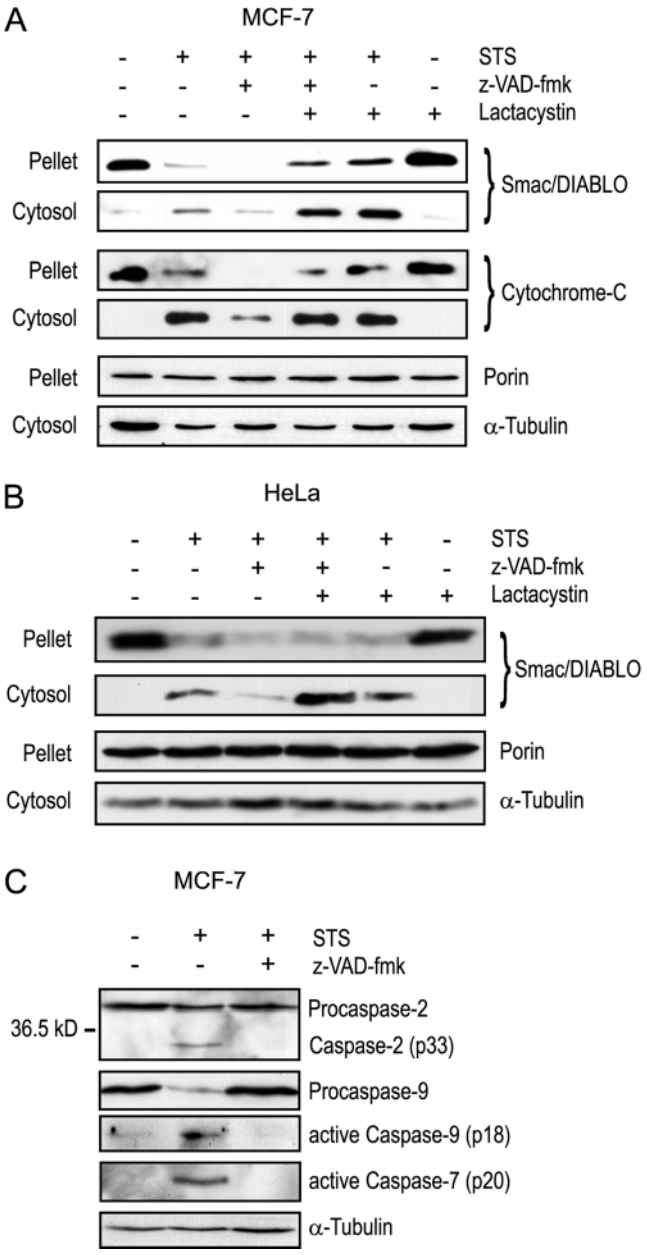

Figure 2. **Effect of caspase and proteasome inhibition on the release of mitochondrial proteins.** (A) Western blot analysis of Casp-3–deficient MCF-7 cells treated with 3 μM STS for 8 h in combination with 200 μM z-VAD-fmk and/or 1 μM of the proteasome inhibitor lactacystin. Release of Smac/DIABLO and cyt-*c* from mitochondria containing pellet fraction into the cytosol was analyzed by Western blotting. Controls were treated with DMSO. α-Tubulin and porin served as control for equal loading of the samples. Experiment was repeated twice with similar results. (B) Western blot analysis of the cytosol and mitochondria-containing pellet fraction of HeLa D98 cells exposed to 3 μM STS for 8 h, either in the absence or presence of z-VAD-fmk or lactacystin. Experiment was repeated with similar results. (C) Western blot analysis demonstrating the processing of caspase-2, -9, and -7 in Casp-3–deficient MCF-7 cells treated with 3 μM STS for 8 h and its inhibition by 200 μM z-VAD-fmk. α-Tubulin served as control for equal sample loading.

enhanced degradation of Smac/DIABLO in STS plus z-VAD-fmk–treated cells observed in the permeabilization/immunoblotting experiments was also reflected by a decreased immunofluorescence brightness in cells that had released Smac/DIABLO. Concomitant redistribution of Smac/DIABLO and cyt-*c* could also be detected in response to TNF-α/CHX (Fig. 1 B). Cells that had released only one of the two intermembrane proteins could not be specifically identified in these experiments. However, in cells that released both proteins, the cyt-*c* immunofluorescence signal appeared frequently more diffuse than the Smac/DIABLO signal. A quantitative immunofluorescence analysis of Smac/DIABLO and cyt-*c* release in MCF-7/Casp-3, MCF-7, and z-VAD-fmk treated MCF-7 cells demonstrated that the level of caspase activation did not influence the occurrence of cyt-*c* or Smac/DIABLO release in response to STS (Fig. 1 C).

Caspase inhibition accelerates a lactacystin-sensitive degradation of Smac/DIABLO

It has been reported previously that Smac/DIABLO is subject to proteasomal degradation (MacFarlane et al., 2002; Hu and Yang, 2003). To investigate whether z-VAD-fmk may promote the degradation of Smac/DIABLO after its release, we treated MCF-7 cells for 8 h with 3 μM STS in the presence or absence of 200 μM z-VAD-fmk or 1 μM of the proteasome inhibitor lactacystin (Fig. 2 A). STS-only treatment induced the cytosolic accumulation of Smac/DIABLO and cyt-*c*, whereas STS plus z-VAD-fmk–treated cultures showed a reduced accumulation of both proteins in the cytosolic fraction, despite complete release from mitochondria. When cells were treated with lactacystin, high amounts of Smac/DIABLO and cyt-*c* reappeared in the cytosolic fraction of STS plus z-VAD-fmk treated cells. A higher cytosolic content of Smac/DIABLO was also observed in STS plus lactacystin- versus STS-only–treated cultures, suggesting that Smac/DIABLO is also partially degraded when caspase activation is not blocked. Similar effects were observed in HeLa D98 cells (Fig. 2 B). z-VAD-fmk–insensitive release of Smac/DIABLO was also observed in MCF-7 cells treated with the topoisomerase II inhibitor Eto (unpublished data).

To investigate which caspases were sensitive to z-VAD-fmk in our experimental setting, we performed an immunoblot analysis of STS- and STS plus z-VAD-fmk–treated MCF-7 cells. Treatment with z-VAD-fmk potently inhibited the processing of initiator caspases 9 and 2, and blocked the formation of the p18 and p20 active subunits of caspases 9 and 7, respectively (Fig. 2 C).

Release of Smac/DIABLO during apoptosis can occur independent of Bax

To investigate whether Bax expression is necessary for the release of Smac/DIABLO from mitochondria, Bax-deficient human DU-145 prostate cancer cells (Honda et al., 2001) were treated with 3 μM STS. The cytosolic accumulation of Smac/DIABLO and cyt-*c* detected after digitonization and immunoblotting. Interestingly, both Smac/DIABLO and cyt-*c* were released from Bax-deficient mitochondria in a similar time course (Fig. 3).

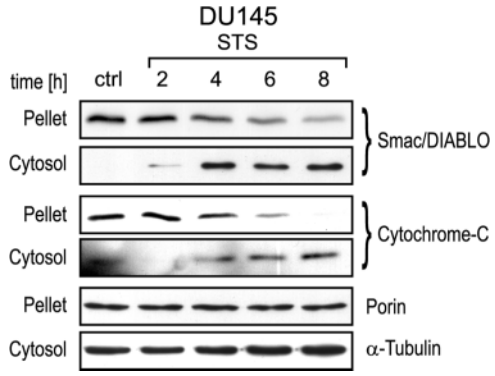

Figure 3. **Release of Smac/DIABLO during apoptosis can occur independent of Bax.** Bax-deficient DU145 cells were treated with 3 μM STS for the indicated time periods. Release of Smac/DIABLO and cyt-*c* from the mitochondria-containing pellet fractions into the cytosol was analyzed by Western blotting. Controls were treated with DMSO. Experiments were repeated twice with similar results.

Characterization of MCF-7 cells expressing a Smac/DIABLO-YFP

To monitor the release of Smac/DIABLO in real-time, we generated MCF-7 and MCF-7/Casp-3 cells expressing a fusion protein comprised of Smac/DIABLO and YFP. Import of Smac/DIABLO-YFP into mitochondria was confirmed by confocal analysis of Smac/DIABLO-YFP fluorescence and its colocalization with the $\Delta\Psi_M$-sensitive dye tetramethyl rhodamine methyl ester (TMRM; Fig. 4 A). We subsequently examined the release behavior of the fusion protein during apoptotic cell death compared with endogenous Smac/DIABLO and cyt-*c*. Immunoblotting experiments were performed with subcellular fractions of transfected MCF-7 cells exposed to 3 μM STS for increasing time periods (Fig. 4 B). The redistribution of Smac/DIABLO-YFP from the mitochondria to the cytosol during apoptosis was similar to that of endogenous Smac/DIABLO and cyt-*c*. Comparable results were obtained in Smac/DIABLO-YFP–expressing MCF-7/Casp-3 cells (unpublished data). Cells that released the Smac/DIABLO-YFP fusion protein in response to STS or TNF-α/CHX also showed a redistribution of Smac/DIABLO immunofluorescence (Fig. 4 C). Similar results were obtained when we analyzed Smac/DIABLO-YFP fluorescence and cyt-*c* immunofluorescence redistribution during apoptosis (Fig. 4 D). Hence, this system enabled one to reliably monitor Smac/DIABLO release at the single cell level during apoptosis.

Real-time single cell analysis of Smac/DIABLO-YFP and cyt-*c*-GFP release demonstrates differences in the kinetics, but not in the onset of release

We monitored individual MCF-7 cells expressing either Smac/DIABLO-YFP or a cyt-*c*-GFP fusion protein (Luetjens et al., 2001; Dussmann et al., 2003a,b) by time lapse confocal microscopy during STS-induced apoptosis. As reported previously, individual cells released cyt-*c*-GFP at different time points after addition of the proapoptotic agent, and the majority of the cyt-*c*-GFP fusion protein was released in one step that was completed within 10 min (Fig. 5, A and B; Goldstein et al., 2000; Luetjens et al., 2001). The

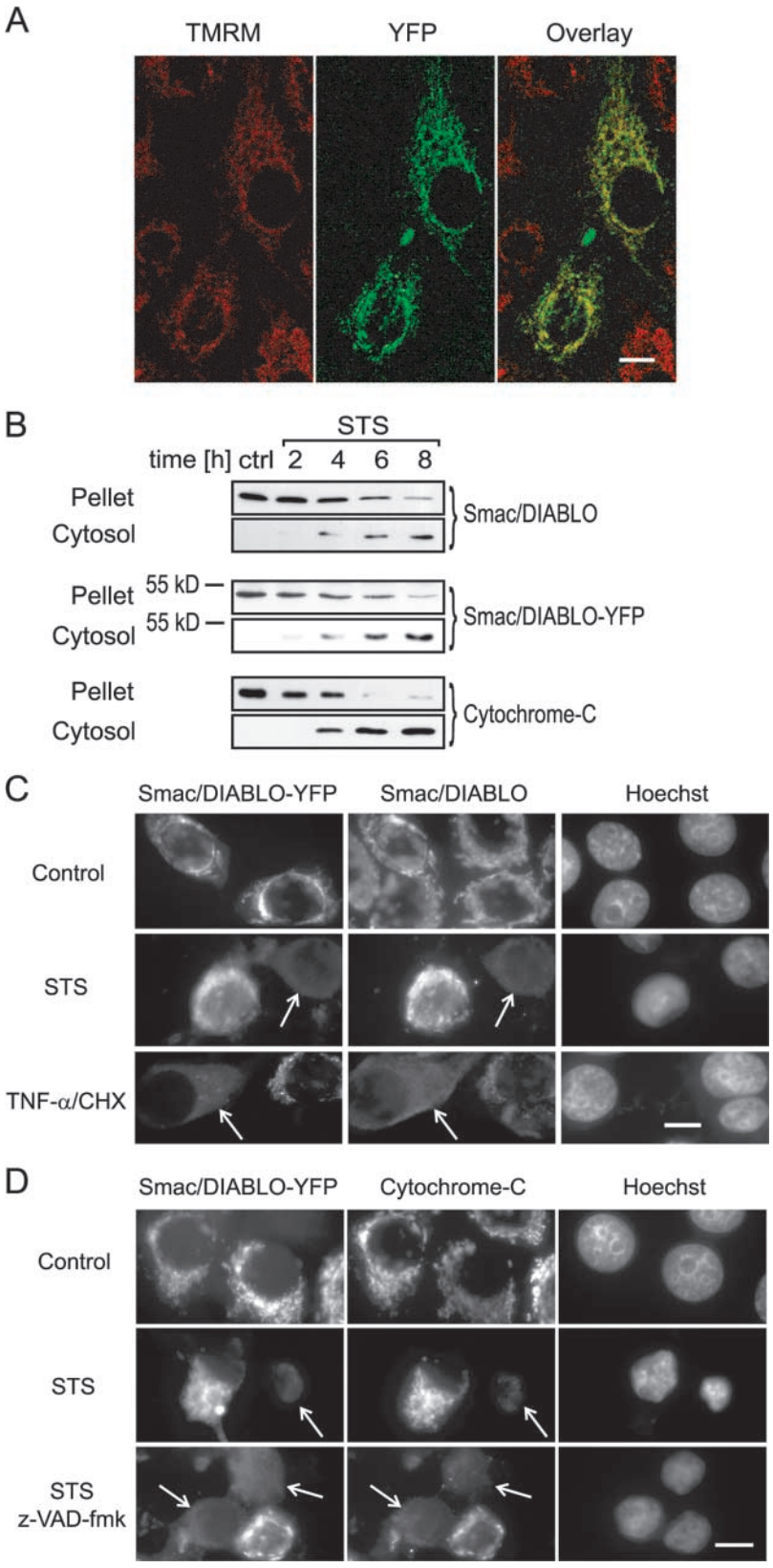

Figure 4. **Characterization of MCF-7 cells expressing Smac/DIABLO-YFP.** (A) Confocal microscopy showing the colocalization of Smac/DIABLO-YFP (green) and TMRM (red) in mitochondria of untreated cells. The overlay image shows yellow pixels at the sites of colocalization. Extended view calculated from three confocal sections with 0.1 μM steps in vertical direction with 0.67 μm resolution and 0.23 μm resolution in horizontal direction. Bar, 10 μm. (B) Western blot analysis of MCF-7 cells stably expressing Smac/DIABLO-YFP. Cells were treated with 3 μM STS for the indicated time periods. Release of Smac/DIABLO, Smac/DIABLO-YFP, and cyt-*c* from the mitochondria-containing pellet fractions into the cytosol was analyzed by Western blotting. Control received DMSO for 8 h. Experiment was repeated twice with similar results. (C) Smac/DIABLO-YFP fluorescence and Smac/DIABLO immunofluorescence of MCF-7 cells treated for 6 h with 3 μM STS or 200 ng/ml and 1 μg/ml TNF-α/CHX. Arrows indicate cells that show a Smac/DIABLO-YFP or Smac/DIABLO redistribution. Control cells received DMSO. Nuclear morphology was detected by Hoechst staining. Bar, 10 μm. (D) Smac/DIABLO-YFP fluorescence and cyt-*c* immunofluorescence of MCF-7 cells treated for 6 h with 3 μM STS or 3 μM STS plus 200 μM z-VAD-fmk. Control cells received vehicle (DMSO). Nuclear morphology was detected by Hoechst staining. Arrows indicate cells that show a Smac/DIABLO-YFP or cyt-*c* redistribution. Bar, 10 μm.

cyt-*c*-GFP redistribution was indicated by a decrease in the standard deviation of the average pixel. Confocal imaging of Smac/DIABLO-YFP redistribution revealed a comparable type of release. The majority of the fluorescence signal was redistributed in a single step, albeit the duration of the Smac/DIABLO-YFP release was significantly increased (Fig. 5, A and C). We simultaneously monitored changes in the mitochondrial uptake of the voltage-sensitive probe TMRM in order to determine the temporal relationship between Smac/DIABLO-YFP, cyt-*c*-GFP release, and mitochondrial

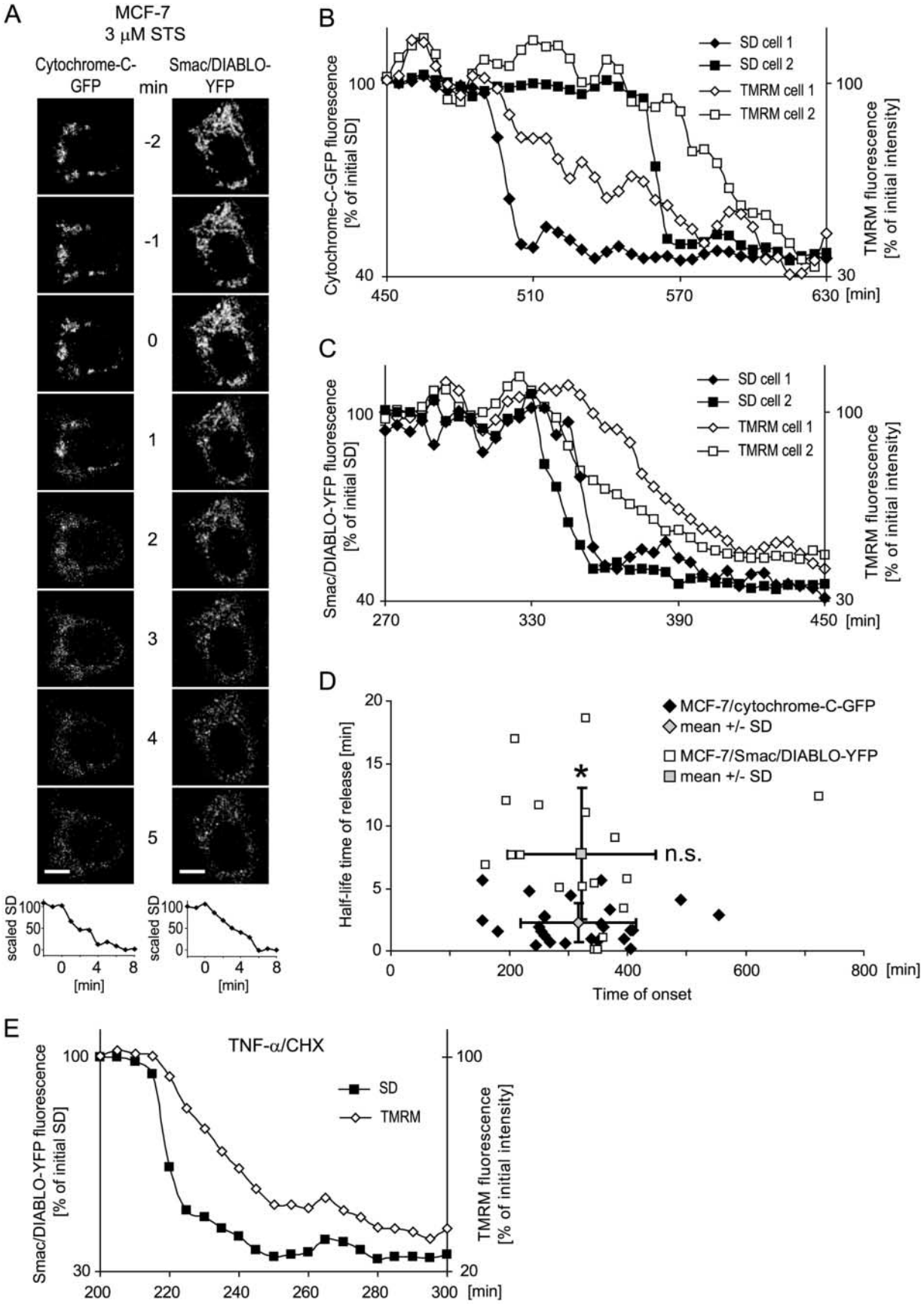

Figure 5. **Comparison of the kinetics and onset of cyt-*c*-GFP and Smac/DIABLO-YFP release in MCF-7 cells.** (A) Confocal image series of two typical cells transfected with cyt-*c*-GFP or Smac/DIABLO-YFP. Both cells show a redistribution of the fluorescence signal in response to 3 μM STS. The onset of release was set to time point zero. The individual traces of the standard deviation of the pixel intensities for the two

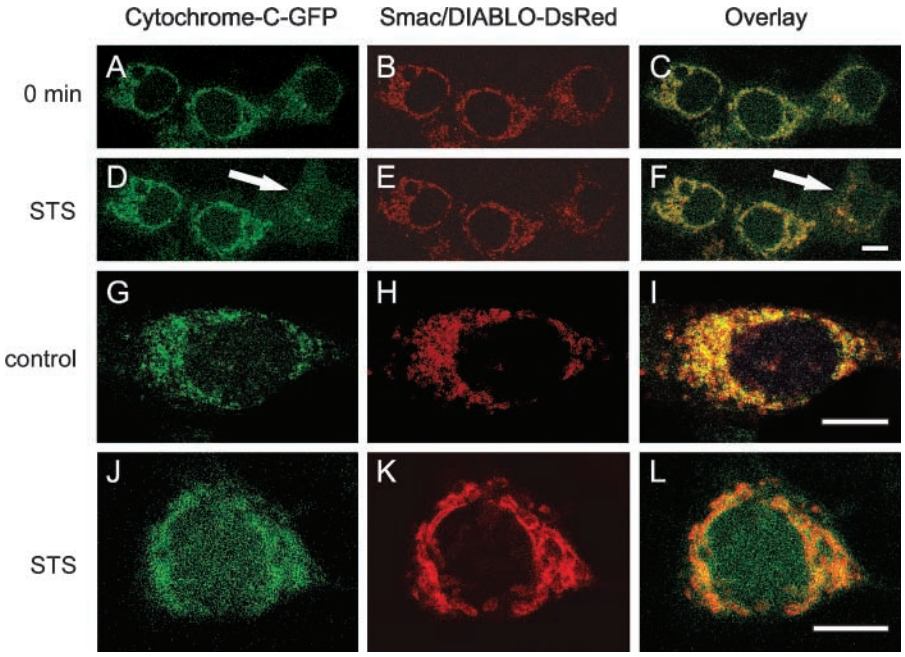

Figure 6. **Smac/DIABLO-DsRed is not released from mitochondria.** MCF-7 cells cotransfected with cyt-*c*-GFP and Smac/DIABLO-DsRed before (A–C) and 40 min after (D–F) an exposure to 3 μM STS. The cell indicated by arrows released cyt-*c*-GFP, but retained its mitochondrial Smac/DIABLO-DsRed signal. Similar results were obtained in 16 cells from three separate time-lapse experiments. Bar, 10 μm. High resolution image of an MCF-7 control cell (G–I) and an MCF-7 cell treated for 6 h with 3 μM STS (J–L). Note the redistribution of cyt-*c*-GFP into the cytosol and nucleus after STS treatment, whereas Smac/DIABLO-DsRed fluorescence retained in mitochondria. Bar, 10 μm.

dysfunction during apoptosis. In both cases, release of cyt-*c*-GFP and Smac/DIABLO-YFP coincided with $\Delta\Psi_M$ depolarization indicated by a decrease in mitochondrial TMRM uptake (Fig. 5, B and C). This suggested that cyt-*c*-GFP and Smac/DIABLO-YFP are released at a similar time point during STS-induced apoptosis.

A quantitative analysis of the onset of cyt-*c*-GFP and Smac/DIABLO-YFP release in response to STS confirmed our observation that there was no significant difference in the onset of release (Fig. 5 D). However, the average duration of the Smac/DIABLO-YFP release, calculated as half-life time, was significantly prolonged 3.4-fold when compared with cyt-*c*-GFP (Fig. 5 D). Similar Smac/DIABLO-YFP release kinetics were observed when apoptosis was triggered by an activation of death receptors (Fig. 5 E).

A Smac/DIABLO-DsRed tetramer is not released from mitochondria

The difference in release kinetics of cyt-*c*-GFP and Smac/DIABLO-YFP could be size dependent. To test this hypothesis further, we generated a Smac/DIABLO-DsRed fusion protein that was readily imported into mitochondria of MCF-7 cells judged by the colocalization with cyt-*c*-GFP (Fig. 6, A–C and G–I). As DsRed is only fluorescent as a tetramer (Baird et al., 2000), the size of the red emitting Smac/DIABLO–DsRed complex is ~188 kD. Time-lapse confocal imaging experiments of MCF-7 cells cotransfected with Smac/DIABLO-DsRed and cyt-*c*-GFP revealed that treatment with 3 μM STS triggered the release of cyt-*c*-GFP, whereas Smac/DIABLO-DsRed retained in mitochondria (Fig. 6, D–F and J–L). Absence of Smac/DIABLO-DsRed release was observed in 16 out of 16 cyt-*c*-GFP release-positive cells in three separate time-lapse experiments.

Casp-3 and z-VAD-fmk–sensitive caspases are not required for a rapid and complete release of Smac/DIABLO-YFP during STS-induced apoptosis

Our digitonization/immunoblotting and immunofluorescence experiments suggested that the release of Smac/DIABLO from mitochondria during STS-induced apoptosis was not influenced by Casp-3 or z-VAD-fmk–sensitive caspases. However, the possibility remained that significant differences existed at the single cell level, which could not be resolved using the above techniques. Therefore, we analyzed the kinetics of Smac/DIABLO-YFP release in response to STS by time-lapse confocal microscopy in MCF-7/Casp-3 cells, MCF-7 cells, and z-VAD-fmk–treated MCF-7 cells. In parallel, we monitored changes in mito-

cells are shown below. For direct comparison of the release kinetics, traces were scaled from 100 (baseline before release) to 0 (baseline after completion of the release). Bar, 5 μm. (B and C) Individual traces of Smac/DIABLO-YFP– or cyt-*c*-GFP–expressing MCF-7 cells treated with 3 μM STS. The release of Smac/DIABLO-YFP and cyt-*c*-GFP was detected as a reduction in the standard deviation of the YFP or GFP pixel intensity, respectively. Changes in mitochondrial TMRM uptake were calculated by determining the average pixel intensity in the TMRM-sensitive channel. Diamonds and squares indicate corresponding TMRM- and YFP-fluorescence changes of two individual cells. (D) Scatter plot showing the onset of cyt-*c*-GFP (black diamonds) or Smac/DIABLO-YFP (open squares) release in individual cells and their corresponding half-life time of the standard deviation decrease, a measure of the release duration (see Materials and methods). Cells were transfected with either cyt-*c*-GFP or Smac/DIABLO-YFP, treated with 3 μM STS and observed by confocal microscopy. Mean values are represented by a gray diamond or square, respectively (±SD in both dimensions). The duration of the Smac/DIABLO-YFP release was greater than that of cyt-*c*-GFP (*t* test; $P < 0.05$), whereas no significant difference was observed regarding the time point of release onset (*t* test). Data were collected from $n = 18$ and 25 cells in three and five experiments, respectively. Asterisk indicates significance (*t* test); $P < 0.05$; n.s., not significant. (E) Kinetics of Smac/DIABLO-YFP release in MCF-7 cells in response to TNF-α/CHX. Individual trace of a typical cell is shown. Similar traces were obtained from $n = 8$ cells in three separate experiments.

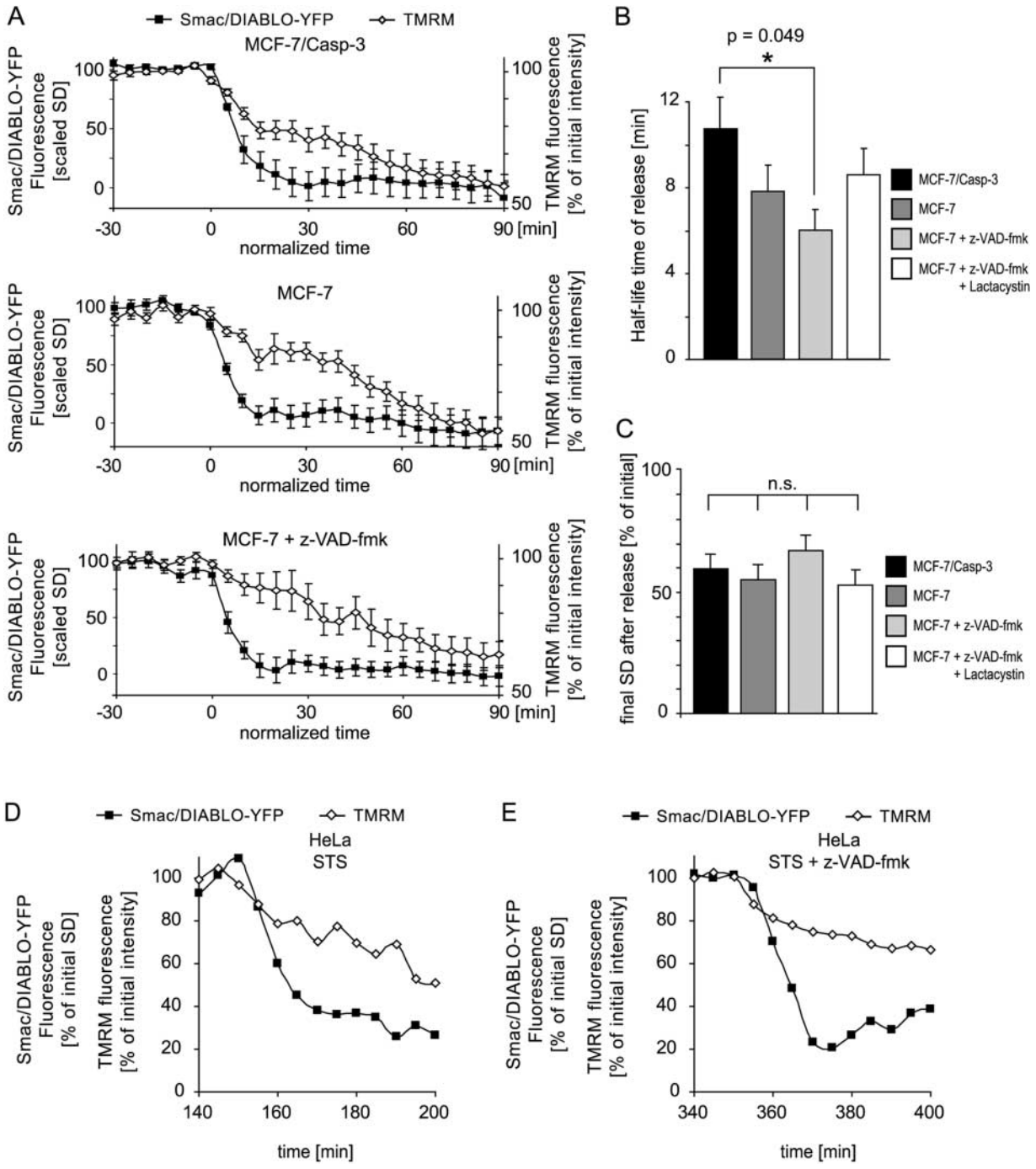

Figure 7. **Casp-3 and z-VAD-fmk–sensitive caspases do not accelerate the kinetics of Smac/DIABLO-YFP release in response to STS.** (A) Quantification of Smac/DIABLO-YFP release and mitochondrial TMRM uptake in cells expressing Smac/DIABLO-YFP. MCF-7/Casp-3 cells, Casp-3–deficient MCF-7 cells and 200 μM z-VAD-fmk–treated MCF-7 cells were equilibrated with 30 nM TMRM and treated with 3 μM STS. Mean traces were calculated from single cell kinetics synchronized to the time of Smac/DIABLO-YFP release. For direct comparison of the release kinetics, traces were scaled from 100 (baseline before release) to 0 (baseline after completion of the release). Bars, ±SEM. (B) Comparison of Smac/DIABLO-YFP release kinetics. Single cell release kinetics were fitted with an exponential decay function and the corresponding half-life times were calculated. Asterisk indicates significance (ANOVA and Tukey test). Error bars, ±SEM. (C) Comparison of the mean standard deviation baseline value reached after completion of the Smac/DIABLO-YFP redistribution. Data in A–C were collected from 9 to 18 cells in three to seven independent experiments per treatment. n.s. , not significant. (D and E) Release of Smac/DIABLO-YFP in HeLa D98 cells. Cells were treated with 3 μM STS in the absence (D) or presence (E) of 200 μM z-VAD-fmk. Individual traces of typical cells are shown. Similar traces were obtained from $n = 29$ and 15 cells in two separate experiments per treatment.

chondrial TMRM uptake, indicative of $\Delta\Psi_M$ depolarization. Confocal imaging of Smac/DIABLO-YFP fluorescence redistribution revealed that the majority of Smac/DIABLO-YFP was released in one single step, regardless of the level of caspase activation (Fig. 7 A). Moreover, the release was always associated with a decrease in mitochondrial TMRM uptake. To calculate the average kinetics of Smac/DIABLO-YFP release, cells were synchronized to the time

of Smac/DIABLO-YFP release (Fig. 7 A). Analysis of the half-life time of the release indicated no significant differences besides a modest difference between MCF-7/Casp-3 cells and z-VAD-fmk–treated MCF-7 cells, with faster release kinetics in the z-VAD-fmk–treated MCF-7 cells (Fig. 7 B). This difference was not detected in z-VAD-fmk plus lactacystin cotreated cells (Fig. 7 B). Analysis of the final standard deviation after the Smac/DIABLO-YFP-release indicated no significant differences in the extent of Smac/DIABLO-YFP redistribution, suggesting no differences in the magnitude of release (Fig. 7 C). As shown previously in MCF-7/Casp-3 cells, $\Delta\Psi_M$ depolarized during STS-induced apoptosis until a new steady-state level was reached ($\Delta\Psi_M{}^{-cyt\text{-}c}$; Dussmann et al., 2003b). z-VAD-fmk–treated MCF-7 cells showed an increased TMRM uptake when $\Delta\Psi_M{}^{-cyt\text{-}c}$ was reached, an effect largely attributable to caspase-dependent plasma membrane potential depolarization (Dussmann et al., 2003b).

We also observed comparable Smac/DIABLO-YFP release kinetics in STS- and STS plus z-VAD-fmk–treated HeLa D98 cells (Fig. 7, D and E), confirming our observations in a second system.

Single cell fluorescence resonance energy transfer (FRET) analysis demonstrates that Smac/DIABLO-YFP release precedes the activation of DEVDases

Release of cyt-*c* triggers the formation of the caspase-activating apoptosome, a process which in many cell types may be sensitive to IAPs (Holcik and Korneluk, 2001). From a mechanistic point of view, release of Smac/DIABLO during apoptosis could, therefore, represent the rate-limiting step in apoptosome formation. However, it is currently unknown how much time is required for apoptosome formation and subsequent DEVDase activation after the release of Smac/DIABLO. To address this question, we used time-lapse imaging experiments in MCF-7/Casp-3 and MCF-7 cells cotransfected with plasmids coding for Smac/DIABLO-YFP and a recombinant FRET probe. The probe was comprised of CFP, a linker peptide containing the optimal effector caspase-cleavage site (DEVD), and YFP. The DEVD linker peptide of the FRET-fusion protein is cleaved upon activation of DEVDases, resulting in a loss of resonance energy transfer and an increase in the CFP/YFP emission ratio (Tyas et al., 2000; Rehm et al., 2002). We have shown previously that the cleavage of the probe during apoptosis correlated well with the cleavage of endogenous cytosolic or nuclear caspase substrates and the activation of executioner Casp-3 and caspase-7 (Rehm et al., 2002). Fig. 8 A demonstrates CFP/YFP ratio changes and changes in the YFP redistribution in a MCF-7/Casp-3 cell in response to 3 μM STS. The cell initially showed a stable baseline CFP/YFP emission ratio, followed by a rapid cleavage of the FRET probe in <10 min. Of note, the majority of Smac/DIABLO-YFP was released before the onset of the FRET probe cleavage. As reported previously, Casp-3–deficient MCF-7 cells demonstrated significantly slower FRET probe cleavage in response to STS, indicating decreased DEVDase activity (Rehm et al., 2002; Fig. 8 B). Interestingly, in these cells, the entire Smac/DIABLO-YFP release was completed before DEVDase activity could be detected. A quantitative analysis of

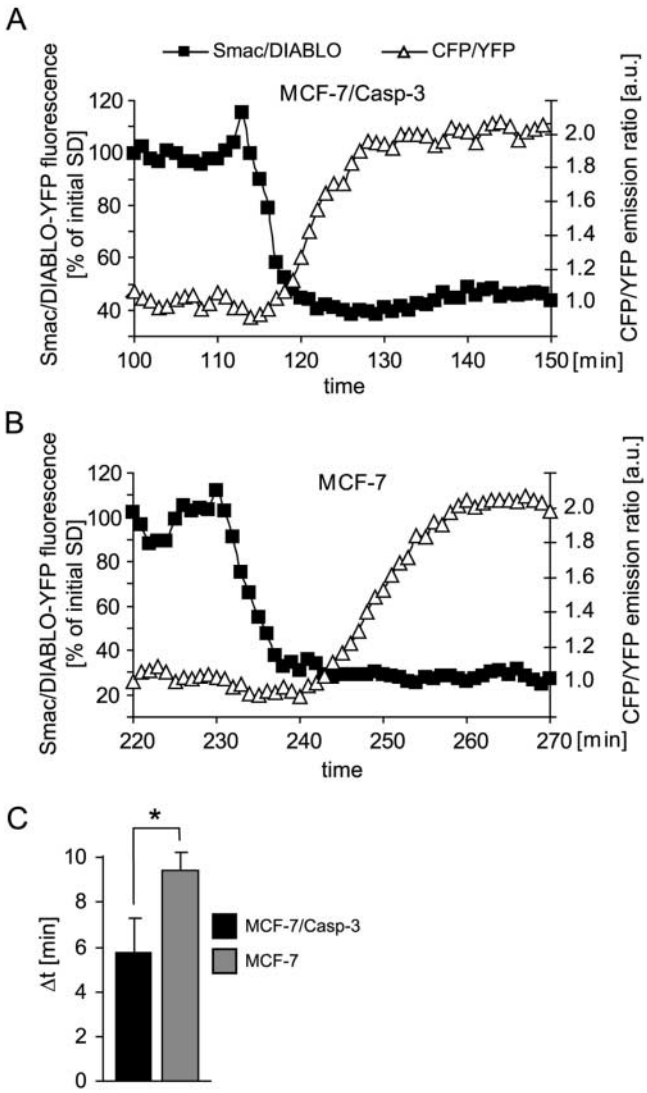

Figure 8. **Smac/DIABLO-YFP release precedes DEVDase activation.** (A and B) Individual traces of a MCF-7/Casp-3 cell and a Casp-3–deficient MCF-7 cell treated with 3 μM STS. The release of Smac/DIABLO-YFP was detected as a reduction in the standard deviation of the YFP pixel intensity. DEVDase activation was measured by proteolytical FRET-disruption of a CFP-DEVD-YFP fusion protein, indicated by an increase in the CFP/YFP emission ratio (see Materials and methods). (C) Statistical analysis of the lag-time between the onset of Smac/DIABLO-YFP release and DEVDase activation (Materials and methods). Data were collected from 9 and 10 cells in four and five individual experiments per treatment, respectively. DEVDase activation was significantly delayed in MCF-7 cells (*t* test, $P < 0.05$). Error bars, ±SEM. Asterisk indicates significance (*t* test); $P < 0.05$.

the time span between release of Smac/DIABLO-YFP and onset of DEVDase activity showed that MCF-7/Casp-3 cells required 5.8 ± 1.5 min for the activation of DEVDases. MCF-7 cells required a significantly longer time period, but surprisingly also achieved efficient DEVDase activity within 10 min (mean value, 9.5 ± 0.8 min; Fig. 8 C).

Discussion

This is the first comprehensive report, which demonstrates, in a defined cellular system, the temporal relationship between mitochondrial cyt-*c* and Smac/DIABLO release,

$\Delta\Psi_M$ depolarization, and effector caspase activation at the single cell level during apoptosis. We demonstrate that the release of large quantities of cyt-*c* and Smac/DIABLO coincides with $\Delta\Psi_M$ depolarization, suggesting that the cause for these three processes is a single event: a significant and fast increase in the outer mitochondrial membrane permeability. Moreover, using the well-established MCF-7 model system, as well as HeLa D98 cells, we demonstrate that neither of these events absolutely requires Casp-3 or z-VAD-fmk–sensitive caspases. Finally, we demonstrate for the first time in living cells that activation of DEVDases occurs within 10 min of mitochondrial membrane permeabilization.

Using standard techniques such as digitonization/immunoblotting and immunofluorescence analysis of Smac/DIABLO and cyt-*c* redistribution, we failed to detect significant differences in the release behavior of the two intermembrane proteins. However, when we used single cell analysis of cyt-*c*-GFP and Smac/DIABLO-YFP release, we noted that Smac/DIABLO-YFP required on average 3.4-fold more time for the release. An earlier study performed in HeLa cells expressing a Smac/DIABLO-GFP fusion protein demonstrated slow release kinetics in response to STS, although a direct comparison with cyt-*c*-GFP release was not performed by the authors (Springs et al., 2002). The differences in the release kinetics between cyt-*c*-GFP and Smac/DIABLO-YFP can be attributable to the difference in size of the proteins. In vitro experiments using reconstituted vesicles have suggested that the release channel of the outer mitochondrial membrane may be very large (>2 MD) and may not discriminate between proteins of different sizes (Kuwana et al., 2002). Our paper suggests that the release may well be size dependent, and that the cut-off of the Smac/DIABLO release channel in vivo may be smaller than ~190 kD. However, we cannot exclude the possibility that different physicochemical properties, such as association with mitochondrial membranes (Du et al., 2000), also play an important role in the different release kinetics.

Of note, our paper demonstrates that the onset of release was not significantly different between Smac/DIABLO-YFP and cyt-*c*-GFP. These observations are supported by recent bulk analyses of permeabilized, tBid-treated HepG2 cells (Madesh et al., 2002), as well as by the Bcl-2 sensitivity of both cyt-*c* and Smac/DIABLO release (Kluck et al., 1997; Yang et al., 1997; Adrain et al., 2001). Hence, Smac/DIABLO and cyt-*c* may show different release and redistribution/degradation kinetics (see Discussion below), yet the cause for the release of both factors is likely to be a rapid, Bcl-2–sensitive increase in the outer mitochondrial membrane permeability.

Using HeLa cells and a well-established model system, the Casp-3–deficient MCF-7 cell line, we demonstrate that Casp-3 and z-VAD-fmk–sensitive caspases were not required for the release of Smac/DIABLO from mitochondria during STS- and Eto-induced apoptosis. Moreover, Casp-3 or z-VAD-fmk–sensitive caspases did not increase the kinetics of Smac/DIABLO-YFP release. Therefore, the release of Smac/DIABLO differs with respect to its caspase dependence from that of apoptosis-inducing factor, which is bound to the mitochondrial inner membrane and may require additional processing for an efficient release and activation during apoptosis (Arnoult et al., 2002; Wang et al., 2002). However, our data suggest that Casp-3 and/or the activity of z-VAD-fmk–sensitive caspases was required to stabilize Smac/DIABLO after its release (Fig. 1 A). This may explain the apparent discrepancy between our paper and the results of Martin and coworkers (Adrain et al., 2001) who investigated cytosolic, but not mitochondrial fractions of daunorubicin-, actinomycin D–, and UV irradiation–treated Jurkat cells in the presence and absence of z-VAD-fmk. In our paper, the proteasome inhibitor lactacystin recovered the cytosolic content of Smac/DIABLO in z-VAD-fmk–treated cells, suggesting that proteasomal activity is responsible for the rapid degradation of released Smac/DIABLO when caspases are inhibited. Interestingly, the proteasome inhibitor likewise increased the cytosolic content of cyt-*c* in STS- plus z-VAD-fmk–treated cells. Two reports have demonstrated that in vitro Smac/DIABLO is subject to proteasomal degradation, and that IAPs function as ubiquitin-protein ligases (E3) in this context (MacFarlane et al., 2002; Hu and Yang, 2003). It is possible that z-VAD-fmk–bound caspases may liberate large amounts of IAPs, which are then able to trigger the degradation of Smac/DIABLO and presumably other proapoptotic factors. However, because cyt-*c* has not been reported to bind to IAPs, our paper suggests that caspases may also generally decrease the ability of cells to degrade or release proteins in a lactacystin-sensitive manner.

Of note, significant amounts of both cyt-*c*-GFP and Smac/DIABLO-YFP were redistributed within a few minutes during apoptosis. In cells that express IAPs or other inhibitors of apoptosome formation, the rate-limiting step in caspase activation may indeed be the release of Smac/DIABLO (Deshmukh et al., 2002; Fulda et al., 2002; Hunter et al., 2003). Our simultaneous analysis of Smac/DIABLO-YFP release and DEVDase activation not only demonstrated that DEVDases activation occurred downstream of the release but also described for the first time the temporal relationship between these two central events during apoptosis. Surprisingly, on average only 5 min were required to actually trigger executioner caspase activity in MCF-7/Casp-3 cells. Significantly more time was required in Casp-3–deficient MCF-7 cells. Still, significant DEVDase activity was already detectable within 10 min of release. Therefore, our data demonstrate an astonishing efficiency of the apoptotic cascade once mitochondria have increased their outer mitochondrial membrane permeability and have established conditions that allow the formation of caspase-activating complexes.

Materials and methods

Materials

Recombinant human TNF-α, CHX, Eto, and embryo-tested mineral oil were purchased from Sigma-Aldrich. STS was from Alexis. The broad-spectrum caspase inhibitor z-VAD-fmk was purchased from Bachem; TMRM was purchased from MobiTec; and lactacystin was purchased from BIOMOL Research Laboratories, Inc.

pSmac/DIABLO-YFP and pSmac/DIABLO-dsRed plasmid preparation

The sequence of Smac/DIABLO was amplified from plasmid pEF mouse DIABLO (Verhagen et al., 2000) by PCR using *Pfu* polymerase. The product was cloned into BglII and KpnI sites of the pEYFP-N1 plasmid or pdsRed-N1 plasmid (CLONTECH Laboratories, Inc.) and subsequently se-

quenced. Oligonucleotide primers were designed to remove the stop codon of the *Smac/DIABLO* gene.

Cell culture and transfection

Human breast adenocarcinoma MCF-7 cells, MCF-7/Casp-3 cells stably transfected with human Casp-3 (Janicke et al., 1998), HeLa D98 cells, and DU145 cells were cultured in RPMI 1640 medium and DME, respectively, (Invitrogen) supplemented with 100 U/ml penicillin, 100 μg/ml streptomycin, and 10% FCS (PAA). Cells were transfected with 0.6 μg of plasmid DNA (pSmac/DIABLO-YFP, pSmac/DIABLO-DsRed, pGFP-N1-cyt-*c* [Heiskanen et al., 1999], pmyc-CFP-DEVD-YFP [Tyas et al., 2000], and 6 μl Lipofectamin reagent [Invitrogen]) per milliliter serum-free culture medium at 37°C for 4 h. For the generation of stable cell lines, transfected cells were selected in the presence of 1 mg/ml G418 for 2 wk and fluorescent clones were enriched. Expression of recombinant proteins was verified by Western blotting. Generation and characterization of MCF-7 cells stably expressing a cyt-*c*-GFP fusion protein have been described previously (Luetjens et al., 2001; Dussmann et al., 2003a). We have shown previously that cyt-*c*-GFP is imported into mitochondria and coreleased with endogenous cyt-*c* after selective outer mitochondrial membrane permeabilization (Luetjens et al., 2001).

Digitonin permeabilization

The release of mitochondrial proteins into the cytosolic compartment was analyzed by selective plasma membrane permeabilization (Luetjens et al., 2001). Extracts were analyzed by Western blot analysis. Control experiments were performed by incubation of untreated cells with permeabilization buffer for 45 min and revealed no release of cyt-*c* and Smac/DIABLO.

Western blotting

Preparation of cell lysates, Western blotting, and immunodetection was performed as described previously (Rehm et al., 2002). Membranes were incubated with a rabbit polyclonal antiactive caspase-9 antibody (MF445, 1:1,000; provided by D.W. Nicholson, Merck Frosst, Point Claire-Dorval, Quebec, Canada), a rabbit polyclonal antiactive p20 caspase-7 antibody (1:1,000; New England Biolabs, Inc.), a mouse monoclonal antiactive caspase-2 antibody (1:1,000; BD Biosciences), a mouse monoclonal antiporin antibody (1:1,000; Calbiochem), a mouse monoclonal anti–α-tubulin antibody (clone DM 1A; 1:5,000; Sigma-Aldrich), a rabbit polyclonal anti–human Smac/DIABLO antibody (1:5,000; R&D Systems), or a mouse monoclonal anti–cyt-*c* antibody (clone 7H8.2C12, 1:1,000; Becton Dickinson). The anti-Smac/DIABLO antibody detected both human and mouse Smac/DIABLO as confirmed with purified mouse Smac/DIABLO expressed as COOH-terminal His_6-fusion protein in *E. coli*.

Immunofluorescence analysis

For immunofluorescence analysis, cells were fixed on 8-well tissue culture slides, washed three times with PBS, permeabilized at 4°C in PBS containing 0.1% Triton X-100 for 3 min, and incubated with blocking solution (PBS with 5% horse serum and 0.3% Triton X-100) at room temperature for 30 min. Cyt-*c* was detected using a monoclonal antinative cyt-*c* antibody (clone 6H2.B4, 1:1,000; Becton Dickinson), or the polyclonal anti-Smac/DIABLO antibody (1:5,000). Antibodies were diluted in PBS containing 1% horse serum and 0.3% Triton X-100. After incubation at room temperature for 2 h, cells were washed twice with PBS and incubated with biotin- or Texas red–conjugated anti–mouse or anti–rabbit IgG antibody (Vector Laboratories) diluted 1:500. The biotin-conjugated secondary antibody was detected using Oregon green–conjugated streptavidin (Molecular Probes) diluted 1:1,000 in PBS for 20 min at room temperature. Epifluorescence microscopy was performed as described below. Chromatin condensation and fragmentation were visualized by nuclear staining with 1 μg/ml of the DNA-binding fluorescent dye Hoechst 33258 (Sigma-Aldrich).

Time-lapse epifluorescence microscopy and digital imaging

Cells were cultivated on 35-mm glass-bottom dishes (Willco BV) in 150 μl medium for at least overnight to let them attach firmly. Cells were treated with the indicated concentrations of proapoptotic drugs in Hepes-buffered medium (10 mM, pH 7.4), covered with embryo-tested mineral oil, and placed in a heated (37°C) chamber (Minitüb) that was mounted on the microscope stage. Fluorescence was observed using an inverted microscope (model TE 300; Eclipse) and a 40× S-Fluor oil objective (Nikon) equipped with a polychroic mirror and filterwheels in the excitation and emission light path containing the appropriate filter sets (polychroic mirror with >50% reflexion from the UV to 443 nm, between 487 and 520 nm, and between 590 and 640 nm; CFP, excitation 436 ± 10 nm, emission 480 ± 20 nm; YFP, excitation 500 ± 20 nm, emission 535 ± 30 nm; FRET, excitation 436 ± 10 nm, emission 535 ± 30 nm; AHF Analysentechnik). Emission and brightfield images were recorded using a CCD camera (Visicam; Visitron Systems). The imaging setup was controlled by MetaMorph software (Universal Imaging Corp.). During control experiments bleaching of the probe was negligible.

Time-lapse confocal fluorescence microscopy and digital imaging

Cyt-*c*-GFP, Smac/DIABLO-YFP, and TMRM fluorescence was monitored and quantified confocally using an inverted microscope (model IX70; Olympus) attached to a confocal laser scanning unit equipped with a 488-nm argon laser and a 60× oil fluorescence objective (Fluoview; Olympus). Fluorescence transmitted the first dichroic mirror with >90% transmission above 505 nm, was divided with a second dichroic mirror at 550 nm, and detected after transmission of a 510–540-nm bandpass filter (GFP or YFP) or a 565-nm high pass emission filter (TMRM). There was no TMRM fluorescence detectable in the GFP/YFP channel. The cross talk between the average pixel intensity of GFP/YFP in the TMRM channel was <10% of the average pixel intensity in the GFP/YFP channel. The maximum change due to GFP/YFP fluorescence in the TMRM channel occurred during the release of the fusion proteins. The resulting change was within the standard deviation of the average pixel intensity of single cells in the TMRM channel (~5%). Fluorescence was detected from a 0.7-μm thick confocal section (full width half maximum).

The membrane-permeant, cationic probe TMRM distributes across cellular membranes according to the Nernst equation. TMRM has little effects on the respiratory chain activity at the concentration used in the present paper (30 nM; Scaduto and Grotyohann, 1999). Saturation of mitochondrial TMRM fluorescence was reached at 250 nM extracellular probe concentration.

For time-lapse imaging, culture dishes were mounted onto the microscope stage that was equipped with a temperature-controlled inlay (model HT200; Minitüb). In control experiments constant fluorescence values were monitored for 24 h in the case of cyt-*c*-GFP and Smac/DIABLO-YFP and 18 h in the case of TMRM. Cells were treated with the indicated concentrations of proapoptotic drugs in Hepes-buffered medium (10 mM, pH 7.4). To prevent evaporation the medium was covered with embryo-tested mineral oil. Image data were obtained using Fluoview 2.0 software (Olympus) and Kalman filtered from three scans for each image.

Cyt-*c*-GFP and Smac/DIABLO-DsRed cotransfected cells were monitored confocally using a microscope (model LSM 510; Carl Zeiss MicroImaging, Inc.) provided with a 63× oil fluorescence objective and a temperature controlled incubation chamber. The confocal laser scanning unit was equipped with a 488-nm argon laser (GFP excitation) and a 543-nm helium/neon laser (DsRed excitation; Carl Zeiss MicroImaging, Inc.). Fluorescence was detected after transmission of a 505–530-nm bandpass filter (GFP emission) or a 560-nm high pass emission filter (DsRed emission).

Kinetics of $\Delta\Psi_M$ depolarization, cyt-*c*-GFP and Smac/DIABLO-YFP release

The quantitative analysis of the fluorescence images was performed using UTHSCSA ImageTool program (University of Texas Health Science Center) and MetaMorph software. For analysis of $\Delta\Psi_M$ kinetics in single cells, the fluorescent mitochondrial regions were segmented from the cytoplasmic and nucleus regions. After background subtraction, the average fluorescence intensity per pixel was calculated. This value resembles the concentration of TMRM inside mitochondria (Dussmann et al., 2003b).

The release kinetics of cyt-*c* or Smac/DIABLO are shown as the standard deviation from the average pixel intensity of individual cells (Goldstein et al., 2000). Compartmentalized cyt-*c*-GFP or Smac/DIABLO-YFP contributes to a high standard deviation and homogeneously distributed cyt-*c*-GFP or Smac/DIABLO-YFP is represented by a low standard deviation. Single cell release kinetics were fitted with the standard exponential decay function and the corresponding half-life times were calculated. For direct comparisons and statistical analyses, single cell standard deviation traces were scaled from 100 (baseline before the release) to 0 (baseline after completion of the release).

Kinetics of FRET disruption

For comparison of onset of Smac/DIABLO release and DEVDase activation, cells were cotransfected with plasmids pSmac/DIABLO-YFP and pmyc-CFP-DEVD-YFP (Tyas et al., 2000; Rehm et al., 2002). Cleavage kinetics were detected at the single cell level by FRET analysis. Images were processed using MetaMorph software. CFP/YFP emission ratios were obtained by dividing the average fluorescence intensity values of single cells after background subtraction. For direct comparisons, single cell traces

were scaled from 1 to 2. The onset of Smac/DIABLO-YFP release was defined as the time point at which the standard deviation of the Smac/DIABLO-YFP signal declined irreversibly below the baseline value minus its standard deviation. The onset of caspase activity was defined as the time point at which the CFP/YFP ratio irreversibly rose above the baseline value plus its standard deviation. The time periods between both events were collected and analyzed statistically.

Statistics

Data are given as means ± SD or SEM. For statistical comparison ANOVA and subsequent Tukey test or *t* test were used. Data that were not standard deviated were analyzed by Mann-Whitney U test. P values smaller than 0.05 were considered to be statistically significant.

We thank Hanni Bähler and Petra Mech for technical assistance, Dr. David L. Vaux (The Walter and Eliza Hall Institute of Medical Research, Australia) for DIABLO cDNA, Dr. Reiner U. Jänicke (University of Düsseldorf, Düsseldorf, Germany), for MCF-7/Casp-3 cells, Dr. D.W. Nicholson for the active caspase-9 antibody, Dr. M. Bähler (Westphalian Wilhems-University, Münster, Germany) for use of the confocal microscope, and Dr. Seamus J. Martin for helpful discussions.

These experiments were supported by a grant from the Interdisciplinary Center for Clinical Research, University Clinics Münster (BMBF 01 KS 9604/0) to J.H.M. Prehn.

Submitted: 18 March 2003
Accepted: 30 July 2003

References

Adachi, S., A. Cross, B. Babior, and R. Gottlieb. 1997. Bcl-2 and the outer mitochondrial membrane in the inactivation of cytochrome c during Fas-mediated apoptosis. *J. Biol. Chem.* 272:21878–21882.

Adrain, C., E.M. Creagh, and S.J. Martin. 2001. Apoptosis-associated release of Smac/DIABLO from mitochondria requires active caspases and is blocked by Bcl-2. *EMBO J.* 20:6627–6636.

Arnoult, D., P. Parone, J.C. Martinou, B. Antonsson, J. Estaquier, and J.C. Ameisen. 2002. Mitochondrial release of apoptosis-inducing factor occurs downstream of cytochrome *c* release in response to several proapoptotic stimuli. *J. Cell Biol.* 159:923–929.

Baird, G.S., D.A. Zacharias, and R.Y. Tsien. 2000. Biochemistry, mutagenesis, and oligomerization of DsRed, a red fluorescent protein from coral. *Proc. Natl. Acad. Sci. USA.* 97:11984–11989.

Cai, J., and D.P. Jones. 1998. Superoxide in apoptosis. Mitochondrial generation triggered by cytochrome c loss. *J. Biol. Chem.* 273:11401–11404.

Chauhan, D., T. Hideshima, S. Rosen, J.C. Reed, S. Kharbanda, and K.C. Anderson. 2001. Apaf-1/cytochrome c-independent and Smac-dependent induction of apoptosis in multiple myeloma (MM) cells. *J. Biol. Chem.* 276: 24453–24456.

Cuvillier, O., V.E. Nava, S.K. Murthy, L.C. Edsall, T. Levade, S. Milstien, and S. Spiegel. 2001. Sphingosine generation, cytochrome c release, and activation of caspase-7 in doxorubicin-induced apoptosis of MCF7 breast adenocarcinoma cells. *Cell Death Differ.* 8:162–171.

Deshmukh, M., C. Du, X. Wang, and E.M. Johnson, Jr. 2002. Exogenous smac induces competence and permits caspase activation in sympathetic neurons. *J. Neurosci.* 22:8018–8027.

Du, C., M. Fang, Y. Li, L. Li, and X. Wang. 2000. Smac, a mitochondrial protein that promotes cytochrome c-dependent caspase activation by eliminating IAP inhibition. *Cell.* 102:33–42.

Dussmann, H., D. Kogel, M. Rehm, and J.H. Prehn. 2003a. Mitochondrial membrane permeabilization and superoxide production during apoptosis. A single-cell analysis. *J. Biol. Chem.* 278:12645–12649.

Dussmann, H., M. Rehm, D. Kogel, and J.H. Prehn. 2003b. Outer mitochondrial membrane permeabilization during apoptosis triggers caspase-independent mitochondrial and caspase-dependent plasma membrane potential depolarization: a single-cell analysis. *J. Cell Sci.* 116:525–536.

Fulda, S., W. Wick, M. Weller, and K.M. Debatin. 2002. Smac agonists sensitize for Apo2L/TRAIL- or anticancer drug-induced apoptosis and induce regression of malignant glioma in vivo. *Nat. Med.* 8:808–815.

Goldstein, J.C., N.J. Waterhouse, P. Juin, G.I. Evan, and D.R. Green. 2000. The coordinate release of cytochrome c during apoptosis is rapid, complete and kinetically invariant. *Nat. Cell Biol.* 2:156–162.

Hegde, R., S.M. Srinivasula, Z. Zhang, R. Wassell, R. Mukattash, L. Cilenti, G. DuBois, Y. Lazebnik, A.S. Zervos, T. Fernandes-Alnemri, and E.S. Alnemri. 2002. Identification of Omi/HtrA2 as a mitochondrial apoptotic serine protease that disrupts inhibitor of apoptosis protein-caspase interaction. *J. Biol. Chem.* 277:432–438.

Heiskanen, K.M., M.B. Bhat, H.W. Wang, J. Ma, and A.L. Nieminen. 1999. Mitochondrial depolarization accompanies cytochrome c release during apoptosis in PC6 cells. *J. Biol. Chem.* 274:5654–5658.

Holcik, M., and R.G. Korneluk. 2001. XIAP, the guardian angel. *Nat. Rev. Mol. Cell Biol.* 2:550–556.

Honda, T., B.T. Gjertsen, K.B. Spurgers, F. Briones, S.J. Lee, M.L. Hobbs, R.E. Meyn, J.A. Roth, C. Logothetis, and T.J. McDonnell. 2001. Restoration of bax in prostate cancer suppresses tumor growth and augments therapeutic cell death induction. *Anticancer Res.* 21(5):3141–3146.

Hu, S., and X. Yang. 2003. Cellular inhibitor of apoptosis 1 and 2 are ubiquitin ligases for the apoptosis inducer Smac/DIABLO. *J. Biol. Chem.* 278:10055–10060.

Hunter, A.M., D. Kottachchi, J. Lewis, C.S. Duckett, R.G. Korneluk, and P. Liston. 2003. A novel ubiquitin fusion system bypasses the mitochondria and generates biologically active Smac/DIABLO. *J. Biol. Chem.* 278:7494–7499.

Janicke, R.U., M.L. Sprengart, M.R. Wati, and A.G. Porter. 1998. Caspase-3 is required for DNA fragmentation and morphological changes associated with apoptosis. *J. Biol. Chem.* 273:9357–9360.

Kluck, R.M., E. Bossy-Wetzel, D.R. Green, and D.D. Newmeyer. 1997. The release of cytochrome c from mitochondria: a primary site for Bcl-2 regulation of apoptosis. *Science.* 275:1132–1136.

Kuwana, T., M.R. Mackey, G. Perkins, M.H. Ellisman, M. Latterich, R. Schneiter, D.R. Green, and D.D. Newmeyer. 2002. Bid, Bax, and lipids cooperate to form supramolecular openings in the outer mitochondrial membrane. *Cell.* 111:331–342.

Li, P., D. Nijhawan, I. Budihardjo, S.M. Srinivasula, M. Ahmad, E.S. Alnemri, and X. Wang. 1997. Cytochrome c and dATP-dependent formation of Apaf-1/caspase-9 complex initiates an apoptotic protease cascade. *Cell.* 91: 479–489.

Liang, Y., C. Yan, and N.F. Schor. 2001. Apoptosis in the absence of caspase 3. *Oncogene.* 20:6570–6578.

Liu, X., C.N. Kim, J. Yang, R. Jemmerson, and X. Wang. 1996. Induction of apoptotic program in cell-free extracts: requirement for dATP and cytochrome c. *Cell.* 86:147–157.

Luetjens, C.M., D. Kogel, C. Reimertz, H. Dussmann, A. Renz, K. Schulze-Osthoff, A.L. Nieminen, M. Poppe, and J.H. Prehn. 2001. Multiple kinetics of mitochondrial cytochrome c release in drug-induced apoptosis. *Mol. Pharmacol.* 60:1008–1019.

MacFarlane, M., W. Merrison, S.B. Bratton, and G.M. Cohen. 2002. Proteasome-mediated degradation of Smac during apoptosis: XIAP promotes Smac ubiquitination in vitro. *J. Biol. Chem.* 277:36611–36616.

Madesh, M., B. Antonsson, S.M. Srinivasula, E.S. Alnemri, and G. Hajnoczky. 2002. Rapid kinetics of tBid-induced cytochrome c and Smac/DIABLO release and mitochondrial depolarization. *J. Biol. Chem.* 277:5651–5659.

Martinou, J.C., and D.R. Green. 2001. Breaking the mitochondrial barrier. *Nat. Rev. Mol. Cell Biol.* 2:63–67.

Martins, L.M., I. Iaccarino, T. Tenev, S. Gschmeissner, N.F. Totty, N.R. Lemoine, J. Savopoulos, C.W. Gray, C.L. Creasy, C. Dingwall, and J. Downward. 2002. The serine protease Omi/HtrA2 regulates apoptosis by binding XIAP through a reaper-like motif. *J. Biol. Chem.* 277:439–444.

Mootha, V.K., M.C. Wei, K.F. Buttle, L. Scorrano, V. Panoutsakopoulou, C.A. Mannella, and S.J. Korsmeyer. 2001. A reversible component of mitochondrial respiratory dysfunction in apoptosis can be rescued by exogenous cytochrome c. *EMBO J.* 20:661–671.

Rehm, M., H. Dussmann, R.U. Janicke, J.M. Tavare, D. Kogel, and J.H. Prehn. 2002. Single-cell fluorescence resonance energy transfer analysis demonstrates that caspase activation during apoptosis is a rapid process. Role of caspase-3. *J. Biol. Chem.* 277:24506–24514.

Scaduto, R.C., Jr., and L.W. Grotyohann. 1999. Measurement of mitochondrial membrane potential using fluorescent rhodamine derivatives. *Biophys. J.* 76: 469–477.

Slee, E.A., M.T. Harte, R.M. Kluck, B.B. Wolf, C.A. Casiano, D.D. Newmeyer, H.G. Wang, J.C. Reed, D.W. Nicholson, E.S. Alnemri, et al. 1999. Ordering the cytochrome *c*–initiated caspase cascade: hierarchical activation of caspases-2, -3, -6, -7, -8, and -10 in a caspase-9–dependent manner. *J. Cell Biol.* 144:281–292.

Springs, S.L., V.M. Diavolitsis, J. Goodhouse, and G.L. McLendon. 2002. The kinetics of translocation of Smac/DIABLO from the mitochondria to the cytosol in HeLa cells. *J. Biol. Chem.* 277:45715–45718.

Suzuki, Y., Y. Imai, H. Nakayama, K. Takahashi, K. Takio, and R. Takahashi.

2001. A serine protease, HtrA2, is released from the mitochondria and interacts with XIAP, inducing cell death. *Mol. Cell.* 8:613–621.

Tyas, L., V.A. Brophy, A. Pope, A.J. Rivett, and J.M. Tavare. 2000. Rapid caspase-3 activation during apoptosis revealed using fluorescence-resonance energy transfer. *EMBO Rep.* 1:266–270.

Verhagen, A.M., P.G. Ekert, M. Pakusch, J. Silke, L.M. Connolly, G.E. Reid, R.L. Moritz, R.J. Simpson, and D.L. Vaux. 2000. Identification of DIABLO, a mammalian protein that promotes apoptosis by binding to and antagonizing IAP proteins. *Cell.* 102:43–53.

Verhagen, A.M., J. Silke, P.G. Ekert, M. Pakusch, H. Kaufmann, L.M. Connolly, C.L. Day, A. Tikoo, R. Burke, C. Wrobel, et al. 2002. HtrA2 promotes cell death through its serine protease activity and its ability to antagonize inhibitor of apoptosis proteins. *J. Biol. Chem.* 277:445–454.

Wang, X., C. Yang, J. Chai, Y. Shi, and D. Xue. 2002. Mechanisms of AIF-mediated apoptotic DNA degradation in Caenorhabditis elegans. *Science.* 298: 1587–1592.

Waterhouse, N.J., J.C. Goldstein, O. von Ahsen, M. Schuler, D.D. Newmeyer, and D.R. Green. 2001. Cytochrome *c* maintains mitochondrial transmembrane potential and ATP generation after outer mitochondrial membrane permeabilization during the apoptotic process. *J. Cell Biol.* 153:319–328.

Yang, J., X. Liu, K. Bhalla, C.N. Kim, A.M. Ibrado, J. Cai, T.I. Peng, D.P. Jones, and X. Wang. 1997. Prevention of apoptosis by Bcl-2: release of cytochrome c from mitochondria blocked. *Science.* 275:1129–1132.

Zamzami, N., P. Marchetti, M. Castedo, D. Decaudin, A. Macho, T. Hirsch, S.A. Susin, P.X. Petit, B. Mignotte, and G. Kroemer. 1995. Sequential reduction of mitochondrial transmembrane potential and generation of reactive oxygen species in early programmed cell death. *J. Exp. Med.* 182:367–377.

Zhang, X.D., X.Y. Zhang, C.P. Gray, T. Nguyen, and P. Hersey. 2001. Tumor necrosis factor-related apoptosis-inducing ligand-induced apoptosis of human melanoma is regulated by smac/DIABLO release from mitochondria. *Cancer Res.* 61:7339–7348.

Zou, H., W.J. Henzel, X. Liu, A. Lutschg, and X. Wang. 1997. Apaf-1, a human protein homologous to *C. elegans* CED-4, participates in cytochrome c-dependent activation of caspase-3. *Cell.* 90:405–413.